Analysis methods used and planned for VIP-2

Alessio Porcelli[1,2,*], *Sergio* Bartalucci[2], *Sergio* Bertolucci[3], *Massimiliano* Bazzi[2], *Mario* Bragadireanu[2,4], *Cesidio* Capoccia[2], *Michael* Cargnelli[1], *Alberto* Clozza[2], *Catalina* Curceanu[2], *Luca* De Paolis[2], *Raffaele* Del Grande[5,2], *Carlo* Fiorini[6], *Carlo* Guaraldo[2], *Mihai* Iliescu[2], *Matthias* Laubenstein[7], *Johann* Marton[1], *Marco* Miliucci[2], *Edoardo* Milotti[8], *Fabrizio* Napolitano[2], *Kristian* Piscicchia[9,2], *Alessandro* Scordo[2], *Hexi* Shi[1], *Diana Laura* Sirghi[2,4], *Florin* Sirghi[2,4], *Francesco* Sgaramella[2], *Oton* Vazquez Doce[2,5], and *Johann* Zmeskal[1]

[1]Stefan Meyer Institute for Subatomic Physics, Kegelgasse 27, 1030 Wien, Austria
[2]INFN, Laboratori Nazionali di Frascati, Via E. Fermi 54, I-00044 Frascati(RM), Italy
[3]Dipartimento di Fisica e Astronomia, Università di Bologna and INFN—Sezione di Bologna, Via Irnerio 46, I-40126 Bologna, Italy
[4]Horia Hulubei National Institute of Physics and Nuclear Engineering, Str. Atomistilor No. 407, P.O. Box MG-6 Buchares-Magurele, Romania
[5]Excellence Cluster Universe, Technische Universität München, Boltzmannstraße 2, 85748 Garching bei München, Germany
[6]Politecnico di Milano, Dipartimento di Elettronica, Informazione e Bioingegneria and INFN Sezione di Milano, I-20133 Milano, Italy
[7]INFN, Laboratori Nazionali del Gran Sasso, Via G. Acitelli 22, I-67100 Assergi - L'Aquila, Italy
[8]Dipartimento di Fisica, Università di Trieste and INFN—Sezione di Trieste, Via Valerio, 2, I-34127 Trieste, Italy
[9]Centro Ricerche Enrico Fermi—Museo Storico della Fisica e Centro Studi e Ricerche "Enrico Fermi", Via Panisperna 89a, 00184 Roma, Italy

Abstract. VIP-2 (VIolation of Pauli exclusion principle - 2) is an underground experiment sited in the underground "Laboratori Nazionali del Gran Sasso." It aims to investigate possible violations of the Pauli Exclusion Principle (PEP) and, in this context, Quantum Gravity models implying violations of PEP. While an upper limit of PEP violation probability is recently published, the data requires further developments of accurate analysis techniques and methods. In this contribution, we present an overview of the methodologies proposed for current and planned analysis.

1 Introduction

As a fundamental pillar of the quantum mechanics for the stability of atoms, Wolfgang Pauli in 1943 formulated the Pauli Exclusion Principle (PEP). It is a direct implication of the Spin Statistic Theorem (SST) [1]. Particles in the Standard Model are grouped in two categories: the bosons with integer spin and the fermions with half-integer spin. Within Quantum Field Theory (QFT), they transform differently by exchanging identical particles: bosonic states have symmetrical permutations, and fermionic ones have antisymmetrical [2].

*e-mail: alessio.porcelli@oeaw.ac.at

© The Authors, published by EDP Sciences. This is an open access article distributed under the terms of the Creative Commons Attribution License 4.0 (http://creativecommons.org/licenses/by/4.0/).

In a given system of identical particles, transitions are forbidden between different symmetry states by the Messiah-Greenberg superselection rule (MG) [3]. The Pauli exclusion principle prohibits two electrons with the same quantum spin number from simultaneously occupying the same atomic energy level in the system. Consequently, more than two electrons cannot occupy each atomic energy level with the opposite quantum number of spin. In such a way, any atomic transition to an energy level already occupied by two electrons implies a PEP violation. Accordingly to MG, a PEP-violating signal has to be searched in open quantum systems, i.e., by looking for transitions among violating states of a prepared system after introducing particles from outside the considered system. Transitions among anomalous states would occur at the standard rate if the involved particles couple universally to the interaction field. An Open Systems experiment tests PEP violation ([4, 5]) constrained by the MG superselection rule, opening a door for a new physics behind the Standard Model.

VIP-2 (VIolation of Pauli exclusion principle - 2) is an Open Systems experiment testing the Pauli Exclusion Principle (PEP), injecting electrons in copper. It measures copper atomic transitions with high precision X-rays detectors and looks for a PEP-violating Kα transition (2p $\rightarrow$ 1s). The energy of the PEP-forbidden Kα atomic transition (schematized in figure 1) would be shifted by about 300 eV, with respect to the standard one, due to the extra shielding provided by the two electrons in the 1s state of the atom [6].

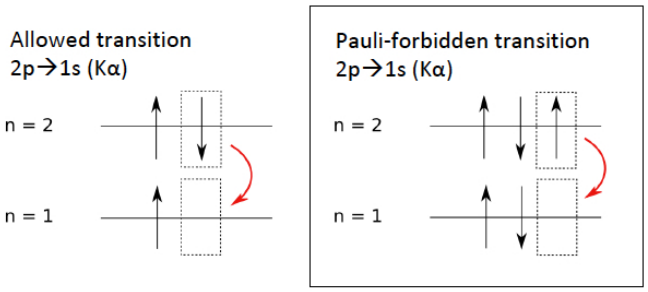

Figure 1. Schematic of PEP-allowed and PEP-violating Kα transition, respectively, on the left and the right.

The number of the PEP-violating emitted X-rays N_x is estimated as follows [7]:

$$N_x \sim \frac{\beta^2}{2} \cdot N_{\text{new}} \cdot \frac{N_{\text{int}}}{10} \cdot \text{efficiency} \,, \tag{1}$$

where $\beta^2/2$ is the PEP-violating probability, N_{new} is the total number of "new" conduction electrons injected into the system, the factor 1/10 is an estimate of the capture probability (per scattering) into the 2p state, N_{int} is the minimum number of electron-atom interactions as electrons flow in the target, and the "efficiency" takes into account both the solid angle covered by the detector and the X-ray absorption in the copper strip.

The goal of the VIP-2 experiment is to improve the upper limit on the Pauli exclusion principle violation probability $\beta^2/2 < 4.7 \times 10^{-29}$, previously set by the VIP experiment, by two orders of magnitude. We present the VIP-2 analysis methodologies used and planned to achieve the aimed goal in this present work.

VIP-2 is also used in a Closed Systems mode. Recent calculations suggest that spin-statistics violations may emerge naturally in the Quantum Gravity models [8, 9], not subject to the MG superselection rule. Consequently, they can also be tested using this configuration without introducing test particles from outside the system. The VIP-2 collaboration has recently undertaken an effort in this direction, but it will not be treated in this work.

2 VIP-2

The VIP-2 experimental apparatus was transported and mounted in the Laboratori Nazionali del Gran Sasso (LNGS) at the end of 2015. Sited beneath the Gran Sasso mountain, the setup is shielded from cosmic rays. The first data-taking campaign started in October 2016 as part of the commissioning phase and ended in November 2017. The detector consisted of two arrays of 1×3 Silicon Drift Detectors (SDDs) surrounding the copper target, each array with 3 cm^2 of the effective surface. The experimental setup was further upgraded in April 2018, when the detector system was replaced with two new arrays, each with 2×8 SDDs, for a total of 32 SDDs. The SDDs are cooled down to about -90 °C. The target system is cooled down by water cooling, keeping them to a temperature of about 12 degrees. When the current of 100 A is turned on, the strips' temperature increases by a few degrees. That induces a temperature rise at the SDDs of the same amount, which does not significantly alter the SDDs' performances. A schematic view of the VIP-2 apparatus is shown in figure 2. Currently published results use the data taken in this configuration.

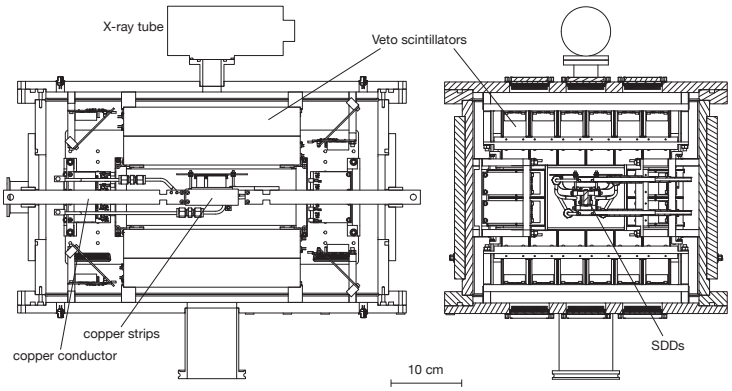

Figure 2. Schematic view of the VIP-2 apparatus installed inside the vacuum chamber.

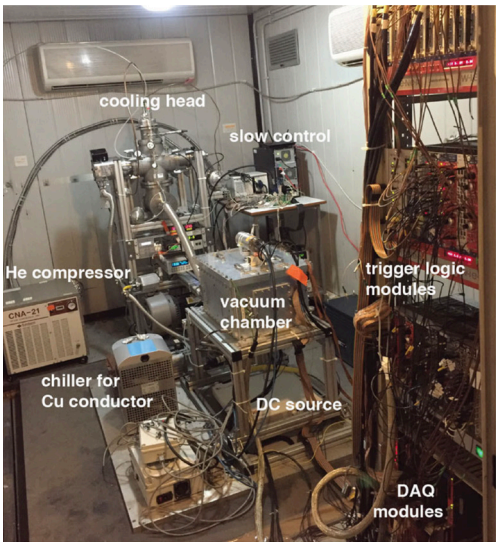

Figure 3. Picture of VIP-2 setup at the LNGS, before the shielding mounting. The apparatus in figure 2 is inside the vacuum chamber in the center of the image.

In November 2018, the setup was surrounded by a passive shielding complex composed of an external lead and inner copper layers, suppressing most of the background due to environmental radiation. More details on the VIP-2 setup, the trigger logic, data acquisition,

and slow control can be found in [6, 10]. The VIP-2 Open Systems experimental setup is acquiring data in this final configuration (figure 3).

3 Analysis

The measured energy spectrum consists of a baseline and a Gaussian distribution for every emission peak (figure 4). The expected Kα emission signals from the Nickel (Ni) and the Copper (Cu) are 7478.2 and 8047.8 eV. The emissions have secondary lines, with a relative amplitude of 51% of the dominant one. These peaks are at 7460.9 and 8027.8 eV respectively for Ni and Cu, a relative shift of 17.3 and 20 eV from their main peak. For VIP-2 purposes, the "background" spectrum is the only signal expected without any current. A new Gaussian is expected when the current is injected: the X-ray emission from the PEP violating states. Its peak is expected at 7746.73 eV with the same width of Kα Cu since subjected approximately to the same electronic noise [6]. The signal's amplitude is proportional to the current injected since it increases the number of interactions electron-atom. However, it is expected to be negligible. Hence, the measurement aims to set the most stringent upper limit. Because of this delicate goal, we have different analysis approaches with both Frequentist and Bayesian inferences. In all methods, the selected energy region of interest for the analysis is from 7000 to 8500 eV, and we test deviation from the standard Kα transition in copper.

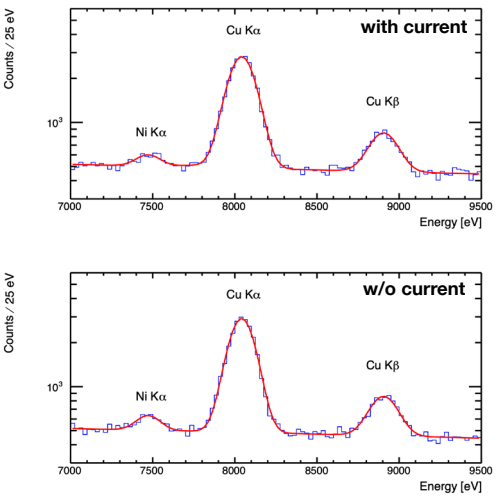

Figure 4. Spectrum of the signal in an energy region where the Kα from Cu and Ni and the Cu Kβ are visible. Above, with current; below without current and purely background. The red lines fit the spectra: the "with current" case also includes the Gaussian of the PEP-violation peaked at 7746.73 eV. See Sect. 3.1.2.

3.1 Frequentist Inference

Frequentist inference is the most classical approach. The paradigm is to extract the model parameters from counts, i.e., the best estimator of parameters θ given the "data" $E(\theta \,|\, \text{data})$. The "data" is assumed close enough to the asymptotic ideal distribution; hence, the inference holds for "large enough" statistics. We use two different methods: Spectra Subtraction (Sect. 3.1.1) and Simultaneous Fit (Sect. 3.1.2).

3.1.1 Spectra Subtraction

The most direct approach is simply subtracting the spectrum measured without (w/o) current from the one with current, both normalized by their time exposure (figure 5, left). If a PEP

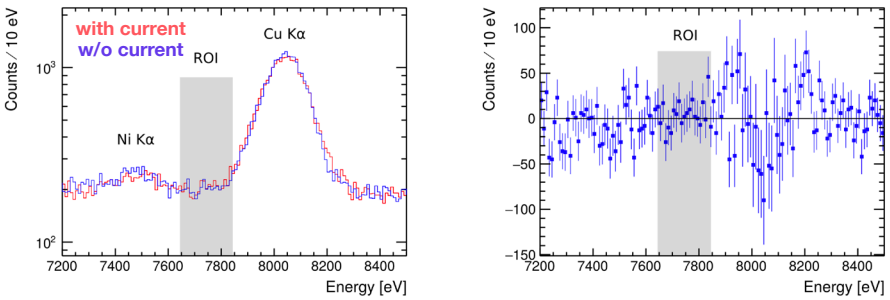

Figure 5. Left: normalized spectra with (red) and without (blue) current in comparison. Right: spectra difference "with" – "without" current. In both, the Region Of Interest is in evidence as a gray band.

violation occurs, some excess must be found in the Region Of Interest (ROI), where the signal is expected (figure 5, right). The ROI is defined as the Full-Width Half Maximum (FWHM) of the expected signal (i.e., the Cu Kα resolution) centered to the signal's peak: from 7647 to 7847 eV. From figure 5, the statistical uncertainty is too large to observe any excess in the ROI. However, this uncertainty lets us set an N_x and determine an upper limit to $\beta^2/2$. We typically show it at 99.7% Confidence Level (C.L.).

3.1.2 Simultaneous Fit

A more performing method consists of a simultaneous fit of the spectra collected with and without current. The two data are characterized by the same background shape, described as equation (2); the spectrum acquired with the current has one more component described by equation (3):

$$f_B(E) = p_0 + p_1 E + p_3 \left[e^{-\frac{(E-p_4)^2}{2p_5^2}} + 0.51\, e^{-\frac{(E-p_4-17.3)^2}{2p_5^2}} \right] + p_6 \left[e^{-\frac{(E-p_7)^2}{2p_8^2}} + 0.51\, e^{-\frac{(E-p_7-20)^2}{2p_8^2}} \right] \quad (2)$$

$$f_S(E) = p_9\, e^{-\frac{(E-7746.73)^2}{2p_8^2}} . \quad (3)$$

All p_i are the free parameters of the fit, describing the baseline as a linear function and all the emissions as Gaussians (see Sect. 3): parameters describing positions of the standard transitions and resolutions are let be free to vary within the experimental uncertainties around the nominal values. To this end, a refined calibration procedure and the investigation of the relative systematic uncertainties are under finalization. Once the spectra are normalized by time exposure, simultaneous fit lets us measure p_9. Through it, we determine the $\beta^2/2$ upper limits, typically shown at 99.7% C.L..

3.2 Bayesian Inference

Unlike the frequentist one, this inference assumes ignorance on data abundance or scarcity. Hence, we look not for the best estimator of model parameters θ, but their probability distribution given "data": $P(\theta \,|\, \text{data})$, called the "posterior". From that, Bayes' theorem in our case is

$$P(S\,|\,N_{\text{data}}) = \frac{P(N_{\text{data}}\,|\,S)\cdot P_0(S)}{\int P(N_{\text{data}}\,|\,S)\cdot P_0(S)\,dS}. \tag{4}$$

$P(\text{data}\,|\,S)$ is the likelihood describing the model of the data distribution, the Poissonian

$$P(N_{\text{data}}\,|\,S) = \frac{(B+S)^{N_{\text{data}}}\cdot e^{-(B+S)}}{N_{\text{data}}!} \tag{5}$$

where B is the expected average of the background counts, S is the excess given by the PEP-violating signal and the searched parameter, and N_{data} are data counts acquired with the current where also the searched signal can be found. Finally, the $P_0(S)$ in equation (4) is called the "prior": an *a priori* hypothesis of weights for all possible parameter values. Since we know nothing about S except it cannot be lower than 0 or above previous experiments limit $S^{\max} = 574$ [6], a Heaviside $\theta(S - S^{\max})$ is considered. The final posterior, hence, become

$$P(S\,|\,N_{\text{data}}) = \frac{(B+S)^{N_{\text{data}}}\cdot e^{-(B+S)}\cdot\theta(S-S^{\max})}{\int_0^{S^{\max}}(B+S)^{N_{\text{data}}}\cdot e^{-(B+S)}\,dS}. \tag{6}$$

Equation (6) is a probability distribution, shown in figure 6 as an example; therefore, the estimator upper limit $\bar{S}$ at a given Confidence Level C.L. is the marginalized distribution

$$P(\bar{S}) = \int_0^{\bar{S}} P(S\,|\,N_{\text{data}})\,dS = \text{C.L.}. \tag{7}$$

S is the N_x in equation (1); hence, we use the resulting $\bar{S}$ to calculate the $\beta^2/2$ upper limit.

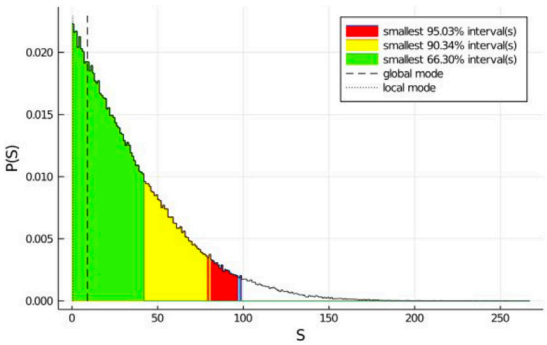

Figure 6. Example of a marginalized distribution for S. Green, yellow and red areas cover the 66.3, 90, and 95% of C.L.s. Data reported are for demonstration only and not meaningful.

The results of this analysis at 90% of C.L. are reported in [11] using data from the first light in the old VIP-2 configuration (see Sect. 2).

We are planning a different model for the present configuration and data set: it will be shown in future publications.

4 Discussion

We have discussed different analysis approaches: each has advantages and disadvantages. The *Spectra Subtraction* (Sect. 3.1.1) is the most direct and rough method, letting the analysis

free from models or assumptions. However, it relies on the definition of an ROI and, more compromising, the statistics in this region: this is not a performing approach for the searched signal but more conservative. It can be used as the most conservative scenario of our results.

The *Simultaneous Fit* (Sect. 3.1.2) does not use any ROI but relies only on modeling the spectrum shape. We are improving its performance using advanced approaches like the CL_s method [12] (not discussed in this work), but the scarcity of the signal compared to the background spectra will always be a limiting factor.

While the Simultaneous Fit is the perfect methodology to cross-check the main approach, *Bayesian Inference* (Sect. 3.2) is our principal analysis method. It is excellent for low statistic signals because it relies more on its model, which is, in our case, simple and measurable. We are currently improving its performance through a different construction of the likelihood.

For the future, we are considering a Machine Learning method. There is a discussion on its potential in improving the results, architecture configuration, and what kind of input we can use (SDDs or background plus signal shapes).

Acknowledgement

This publication was made possible through the support of Grant 62099 from the John Templeton Foundation. The opinions expressed in this publication are those of the authors and do not necessarily reflect the views of the John Templeton Foundation. We acknowledge support from the Foundational Questions Institute and Fetzer Franklin Fund, a donor advised fund of Silicon Valley Community Foundation (Grants No. FQXi-RFP-CPW-2008 and FQXi-MGB-2011), and from the H2020 FET TEQ (Grant No. 766900) and INFN (VIP). We thank the Austrian Science Foundation (FWF) which supports the VIP2 project with the grants P25529-N20, project P 30635-N36 and W1252-N27 (doctoral college particles and interactions). K. P. acknowledges support from the Centro Ricerche Enrico Fermi - Museo Storico della Fisica e Centro Studi e Ricerche “Enrico Fermi” (Open Problems in Quantum Mechanics project).

References

[1] G. Lüders, B. Zumino, Phys. Rev. **110**, 1450 (1958)
[2] C. Curceanu, J. Gillaspy, R. Hilborn, Am. J. Phys. **80**, 561–577 (2012)
[3] A. Messiah, O. Greenberg, Phys. Rev. **136**, B248–B267 (1964)
[4] G. Gentile j, Il Nuovo Cimento **17**, 493–497 (1940)
[5] R. Amado, H. Primakoff, Phys. Rev. C **22**, 1338–1340 (1980)
[6] H. Shi, E. Milotti, S. Bartalucci, M. Bazzi, S. Bertolucci, A. Bragadireanu, M. Cargnelli, A. Clozza, L. De Paolis, S. Di Matteo et al. (VIP), Eur. Phys. J. C **78**, 319 (2018)
[7] E. Ramberg, G. Snow, Phys. Lett. B **238**, 438–441 (1990)
[8] M. Arzano, J. Kowalski-Glikman, Phys. Lett. B **760**, 69–73 (2016)
[9] A. P. Balachandran, T. Govindarajan, G. Mangano, A. Pinzul, B. Qureshi, S. Vaidya, Phys. Rev. D **75**, 045009 (2007)
[10] C. Curceanu (Petrascu), S. Bartalucci, S. Bertolucci, M. Bragadireanu, M. Cargnelli, S. Di Matteo, J. Egger, C. Guaraldo, M. Iliescu, T. Ishiwatari et al., Found. Phys. **41**, 282–287 (2011)
[11] K. Piscicchia, *et al.* (VIP), Entropy **22**, 1195 (2020)
[12] A. Read, Workshop on Confidence Limits **205** (2000)